Effect of δ-phase Precipitation on the Repair Weldability of Alloy 718

M.E. Mehl
Pratt and Whitney
West Palm Beach, FL 33410

J.C. Lippold
The Ohio State University
Columbus, OH 43210

Abstract

The effect of δ-phase precipitation, resulting from multiple weld repair and postweld heat treatment cycles, on the weldability of Alloy 718 was investigated. The liquation cracking susceptibility of both wrought base metal and weld metal from a "retired" turbine engine component was determined using a hot ductility testing procedure. Results of this testing revealed a degradation in weldability resulting from a large volume fraction of δ-phase, and some recovery of weldability when an elevated temperature postweld heat treatment was used.

Superalloys 718, 625, 706 and Various Derivatives
Edited by E.A. Loria
The Minerals, Metals & Materials Society, 1997

Introduction

Alloy 718 is often selected for construction of large gas turbine engine components because of its attractive elevated temperature properties and good fabricability. In particular, Alloy 718 exhibits superior resistance to strain-age cracking (SAC) during postweld heat treatment (PWHT) and is therefore selected for applications that require welding. The resistance to SAC results from a more sluggish precipitation reaction during PWHT, with γ'' forming rather than the γ' precipitate common to many Ni-base superalloys. The BCT γ'' phase is the metastable form of the Ni_3Nb stoichiometry. After extended exposures above 650 °C, the γ'' phase transforms to a stable orthorhombic structure of Ni_3Nb, called δ-phase. [1,2]

For most applications incorporating the wrought form of the material, a conventional PWHT cycle comprised of a 912-954 °C/1 hr. solution treatment followed by aging at 718 °C/8 hrs. plus 621 °C /8-10 hrs. is utilized.[3] Since these temperatures are below the δ solvus, precipitation of δ-phase occurs during PWHT. When numerous exposures to these heat treatments occur (e.g. multiple repair cycles), excessive δ-phase accumulation may result. This accumulation, referred to as "δ-phase embrittlement," has been reported to contribute to the degradation of mechanical properties in Alloy 718 components. [3-7] The use of modified heat treatments with solution temperatures above the δ-solvus can be employed to combat the adverse effect of δ-phase accumulation [3,4], but may negatively affect the fatigue crack growth properties of the material due to grain growth.

The purpose of this investigation was to evaluate the effect of δ-phase on the weldability of Alloy 718. Industrial experience at turbine engine repair facilities suggests that a degradation in the weldability of Alloy 718 occurs in service-exposed components that have undergone multiple repair/PWHT cycles. This is manifested as an increase in apparent liquation cracking during repair welding. The work presented here attempts to quantify this increase in susceptibility using standard weldability test techniques, and to relate this behavior to the microstructure that evolves during service exposure and multiple repair events.

Experimental Procedure

Materials

Wrought Alloy 718 material removed from a "retired" component which had experienced numerous repair and heat treatment cycles was evaluated. For a baseline reference, a wrought heat of virgin-processed Alloy 718 of similar composition to the service-exposed material was also tested. Samples for weldability testing were prepared in a variety of conditions, including wrought base metal and weld metal in both the as-received (i.e. "retired") condition and after PWHT. Table I summarizes the material conditions and designations used in this investigation. PWHT was conducted using a solution temperature of either 912 or 1038 °C (1700 or 1900 °F, per the designations), followed by a 718 °C (1325 °F)/8 hrs. plus 621 °C (1150 °F)/8-10 hrs. aging treatment. The composition of the materials used in this investigation are listed in Table II.

Hot Ductility Testing

The Gleeble hot ductility test was chosen as a weldability testing tool to evaluate the liquation cracking susceptibility of Alloy 718 under various material conditions. A methodology for the

Table I. Material Conditions and Designations

Designation	Description of Condition
Reference	Wrought, virgin-processed heat (fully aged)
BM	Wrought, as-received (retired), solution annealed condition
BM1700	BM, 912°C/15 min. + age cycle
BM1900	BM, 1038°C/15 min. + age cycle
WM	Weld metal, as-received (retired), solution annealed condition
WM1700	WM, 912°C/15 min. + age cycle
WM1900	WM, 1038°C/15 min. + age cycle

interpretation of hot ductility test results formulated by Lin *et al* was used to correlate these results with metallurgical phenomena occurring during actual weld thermal cycles. [8] Hot ductility testing was performed on a Gleeble HAZ 1000® test apparatus. All specimens were tested with a common set of test parameters. Samples were heated to peak temperature at rate of 111 °C/sec, held at peak temperature for 0.03 sec, and cooled at approximately 30 °C/sec to room temperature. Samples were pulled to failure at a rate of 25 mm/sec.

Test specimens were fractured at various temperatures on-heating and on-cooling to determine the ductility response of the material. Ductility was measured as a reduction in area at the fracture surface. Specimens fractured along this thermal excursion enabled a determination of the nil-ductility and ductility-recovery temperatures (NDT and DRT). The nil-strength temperature (NST) for each test group was determined by applying a small tensile load on the specimens while they were heated to the melting temperature range.

Table II. Composition of Materials (wt%)

Condition	Ni	Fe	Cr	Nb	B	S	P	Al	Ti	C	Mo	Mn	Si
Reference	51.7	17.9	20.0	5.41	.006	.001	.001	.49	1.01	.014	2.92	.01	<.10
BM BM1700 BM1900	53.0	18.2	18.1	5.37	.003	.002	.015	.47	1.34	.055	3.00	.17	<.10
WM	51.8	19.4	18.4	5.04	.003	.001	.014	.51	1.03	.046	2.97	.29	.22
WM1700 WM1900	53.7	18.1	18.1	5.35	.003	.001	.015	.50	1.01	.041	2.95	<.10	.11

Metallurgical Evaluation

Samples selected for metallographic examination were polished through 0.05μm alumina and electrolytically etched with a 5% chromic acid solution at 1-2 VDC for 2-5 seconds. Optical microscopy was performed at magnifications up to 400X. The percentage of secondary phases present in the microstructure was analyzed with the OPTIMAS® image analysis software for each of the "starting" microstructures to yield a percent of secondary phases for each test material group. Here, the area fraction is assumed to equal the volume fraction of secondary phases. The scanning electron microscope (SEM) was utilized for high-

magnification observation of the hot ductility test specimens. Selected metallographic samples of hot ductility specimens, especially on-cooling specimens which were thermally cycled to the peak temperature, were carbon-coated and viewed in the SEM. Quantitative elemental analyses of metallographic hot ductility specimens were performed to calculate local compositions at various locations of the on-cooling microstructures. In the SEM, a spot mode of the beam was utilized in conjunction with EDAX software for compositional analysis.

Results

Microstructure of Starting Materials

The service-exposed wrought material contained considerable δ-phase (Figure 1a) as a consequence of numerous PWHT cycles during repair operations. An additional low-temperature (912 °C) solution plus age cycle performed on this material caused only a minor change in microstructure relative to the starting condition. However, the high-temperature (1038 °C) solution plus age cycle imposed on the starting material caused a marked change in the wrought microstructure (Figure 1b) as extensive δ-phase dissolution is apparent when compared to Figure 1a.

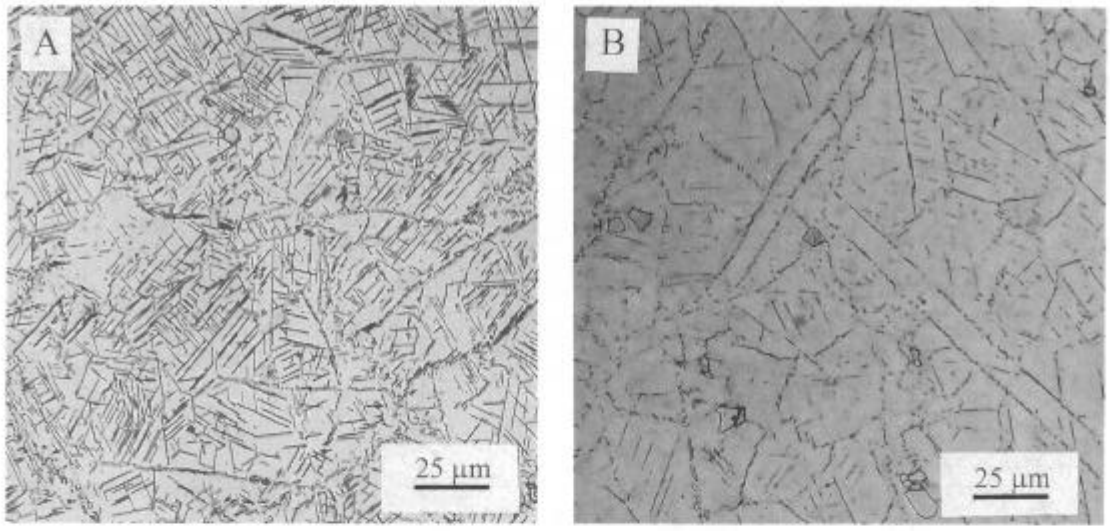

Figure 1. Microstructure of service-exposed wrought Alloy 718, 400X. A) As-received, B) after PWHT at 1038 °C.

The weld metal test group microstructures exhibited a cellular-dendritic solidification morphology typical of the Ni-base alloy system (Figure 2). The as-received weld metal (service-exposed factory assembly weld) had an extensive network of δ-phase around interdendritic Laves-phase constituents (Figure 2a). PWHT at a 912 °C solution temperature dissolved a significant amount of the δ-phase population, but not the Laves. Solution heat treatment at 1038 °C dissolved both the δ-phase and Laves (Figure 2b). The results of the OPTIMAS® measurements for the secondary phase content in the various material conditions are presented in Table III. Note that this data represents all phases present, but is dominated

by the presence of δ-phase in the BM groups. Note that the 1038 °C solution annealing treatment results in significant dissolution of secondary phases in both the base and weld metals.

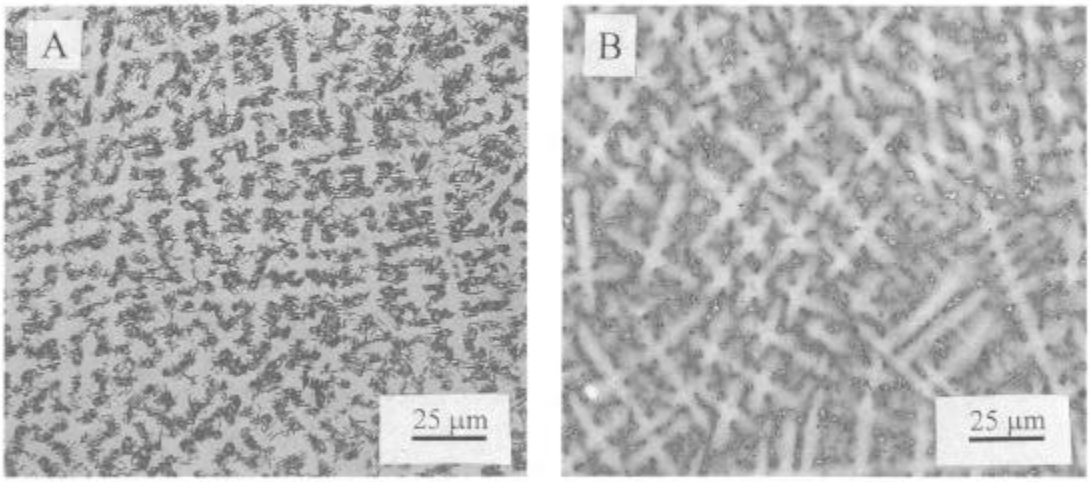

Figure 2. Microstructure of service-exposed Alloy 718 weld metal, 400X. A) As-received, B) after PWHT at 1038 °C.

Table III. Second Phase Content

Condition	Percent Secondary Phases
Reference	16
BM	26
BM1700	26.9
BM1900	8.7
WM	30.5
WM1700	17.8
WM1900	8.1

Hot Ductility Behavior

HAZ liquation cracking susceptibility was quantified by determining the on-cooling liquation cracking temperature range (LCTR), which is defined as the temperature range between the peak temperature and the DRT (T_P - DRT). Within this range, the material exhibits zero ductility and is therefore subject to liquation cracking during weld cooling. The LCTR, NDT, NST, and DRT values for each of the test groups is given in Table IV as determined from hot ductility testing. Note that the LCTR is highest in the weld metal and base metal removed from the retired Alloy 718 hardware. The use of a PWHT with a high solution temperature (1038 °C) is the most effective at reducing liquation cracking susceptibility as measured by the LCTR value. PWHT performed with the lower solution temperature had essentially no effect on the weldability behavior.

Table IV. Hot Ductility Test Results

Condition	NDT (°C)	NST (°C)	DRT (°C)	LCTR (°C)
Reference	1150	1283	1090	170
BM	1145	1301	1070	190
BM1700	1130	1294	1080	180
BM1900	1160	1294	1080	180
WM	1120	1294	1070	190
WM1700	1120	1296	1070	190
WM1900	1140	1271	1090	170

Metallurgical Evaluation

Since HAZ and weld metal liquation cracking are presumed to occur during the cooling portion of a weld thermal cycle, characterization focused on the on-cooling hot ductility samples from each material group. Within the on-cooling regime, specimens in the neighborhood of the DRT from each test group were selected for metallographic and fractographic evaluation. In Figure 3, isolated regions of intergranular liquid, some of which contain Laves-eutectic constituents, are observed in the on-cooling microstructure of the reference heat as a result of the imposed thermal cycle. The fractograph reveals that a mixture of liquid film and ductile features exists at a fracture temperature slightly below the DRT, indicating that solidification of liquid grain boundary films was not complete at this temperature.

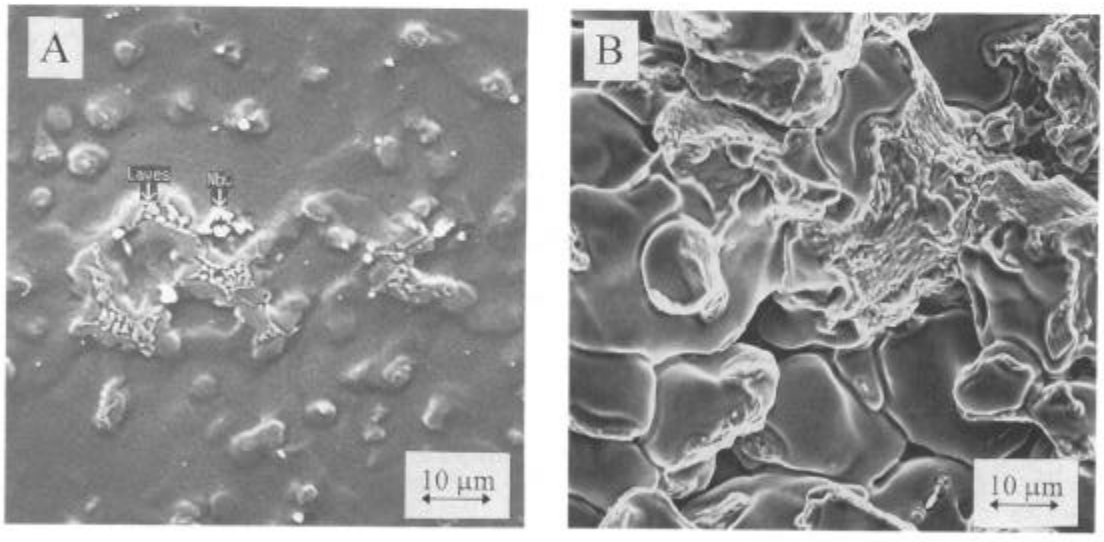

Figure 3. Reference heat on-cooling hot ductility sample heated to a peak temperature of 1260°C and tested at 1080°C. A) SEM micrograph, 1000X, B) fractograph, 1000X.

Similar microstructural features were observed for the service-exposed base metal groups, although the extent of liquation was generally greater in the service-exposed material than for the reference heat. This observation would explain the lower LCTR range reported for the control heat relative to those of the service-exposed base metal groups. The extensive liquation in the BM group reinforces the larger LCTR observed in comparison to the remaining base metal groups. Fracture behavior for these groups exhibited morphologies with a mixture of liquid film and ductile rupture present at the fracture event in the vicinity of the DRT, similar to that observed for the reference heat (Figure 3b).

For the weld metal groups, on-cooling microstructural features differed somewhat from the base metal groups due to the nature of the starting microstructure. For example, in Figure 4 the liquation of interdendritic phases is evident in addition to the more severely liquated weld metal solidification grain boundaries in the WM condition. The liquid distribution is more continuous along the solidification grain boundaries, and formation of eutectic solidification products along the boundaries suggests that terminal solidification occurred in these locations. The WM1900 group (Figure 5) exhibited considerably less liquid formation throughout the microstructure due to the more complete dissolution of the interdendritic phases present as a result of the high solution temperature, and could explain the higher DRT (smaller LCTR) value exhibited by this test group (see Table IV). The fracture features of these groups are quite different from those of the base metal groups observed previously due to the difference of weld metal solidification structure from the base metal.

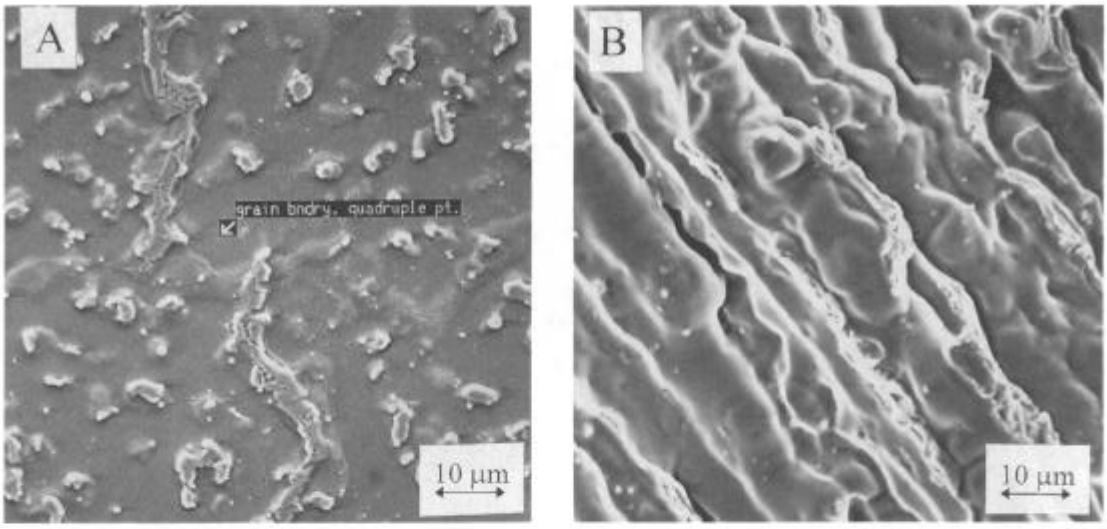

Figure 4. Weld metal (WM) on-cooling hot ductility sample heated to a peak temperature of 1260°C and tested at 1072°C. A) SEM micrograph, 1000X, B) fractograph, 1000X.

The results of the EDS analyses performed at various locations of the on-cooling microstructures for all test groups are given in Table V. The Nb concentration in the matrix, liquid pools, and at the terminal solidification points is presented for each group, and each value is the average of several spot analyses. From this data, it is clearly seen that the Nb concentration is elevated at regions where liquation was observed, especially in the last-to-solidify regions. Segregation of Nb in the starting microstructures would contribute

somewhat to these drastic variations in concentration, but the high concentration of Nb at the terminal solidification points is likely a result of the segregation of Nb during the solidification of liquid films during the cooling portion of the simulated HAZ thermal cycles. As expected, the Nb concentrations were higher in groups which exhibited lower DRT values due to suppression of the solidification temperature. It is noted that these values for Nb concentration may not be considered exact representations of the local Nb content, but serve to illustrate that Nb segregation was more severe in material groups which exhibited larger LCTR values. Limitations of the EDS technique, including the beam spot size and subsurface excitation volume interactions, dictate that some level of error exists in the determination of the Nb concentrations. However, by performing the analysis in several locations for each test region (i.e. matrix, liquid pools, etc.), the amount of experimental error is minimized and would yield a more accurate representation of Nb concentration calculations.

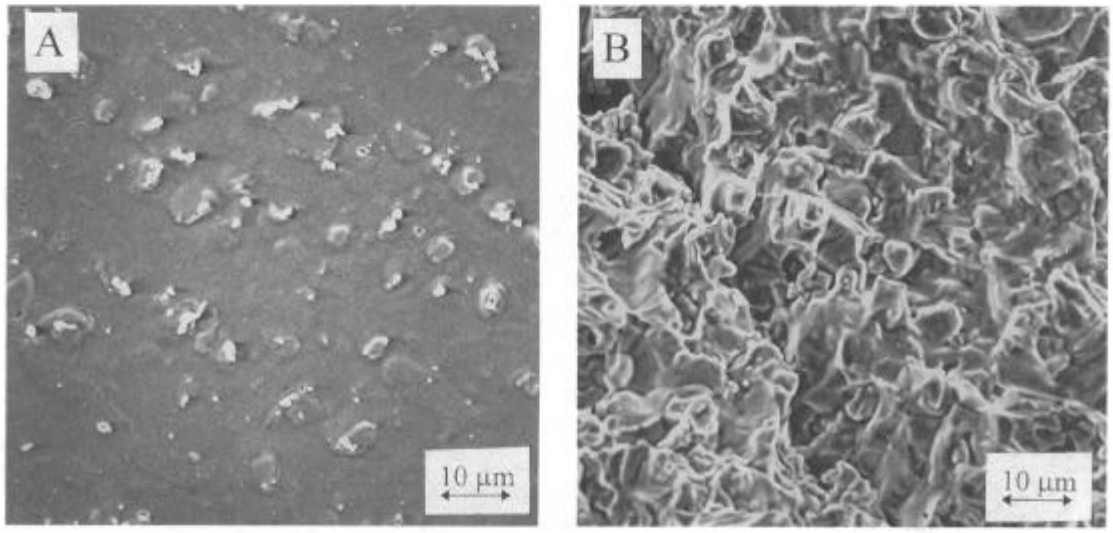

Figure 5. WM/1900 on-cooling hot ductility sample heated to a peak temperature of 1260°C and tested at 1085°C. A) SEM micrograph, 1000X, B) fractograph, 1000X.

Table V: EDS spot analyses of Nb concentration (wt.%) at various locations in on-cooling microstructures from hot ductility specimens.

Condition	Matrix	Liquated region	Eutectic
Reference	6.1	12.0	31.4
BM	5.2	8.6	33.7
BM1700	4.4	10.1	26.6
BM1900	5.9	8.5	26.7
WM	4.4	8.2	28.1
WM1700	4.3	10.4	28.7
WM1900	5.4	10.4	29.7

Discussion

Service-Exposed Material Weldability Degradation

The reported degradation in weldability of Alloy 718 after long-term, high-temperature exposure and multiple repair cycles strongly suggests some relationship with the observed alteration in the microstructure, specifically the accumulation of δ-phase both inter- and intragranularly. Such accumulation of the Nb-rich δ-phase has been found to enrich the grain boundary regions in Nb and deplete the intragranular regions adjacent to the grain boundaries.[9] Such local enrichment in Nb, which is known to adversely affect material weldability by melting point depression, would tend to increase the susceptibility of the material to liquation cracking. This hypothesis is supported by comparing the wrought virgin-processed material to service-exposed wrought base metal (BM group). Figure 1a clearly shows the δ-phase accumulation which has occurred in the service-exposed material. By referring to Table II, it is observed that the control heat has a Nb content slightly higher than that of the service-exposed base metal group (BM), as well as a higher B level (another melting point depressant). From the hot ductility test results presented in Table IV, however, it is noted that a 20°C increase in the on-cooling LCTR occurred in the service-exposed material compared to the virgin-processed program heat material, even though Nb and B levels in the program heat material were elevated. This extension of the on-cooling LCTR represents a notable increase in the susceptibility to liquation cracking for the service-exposed material. Such comparison supports the reported increase in cracking susceptibility by industrial repair facilities for service-exposed Alloy 718 components.

Influence of Heat Treatment and Secondary Phase Content

Table VI lists the hot ductility data generated for the service-exposed material groups in such order to isolate the effects of heat treatment condition on weldability. In addition to the LCTR values generated from hot ductility testing, a column is added for secondary phase content of the starting microstructures for additional evaluation of thermal treatment effects. For the wrought, service-exposed base metal groups, it is observed that only slight variation in weldability amongst the three conditions was encountered from testing, with the starting material demonstrating the poorest weldability.

Table VI. Effect of PWHT on Hot Ductility Behavior

Condition	LCTR	Second Phase (vol %)
Control	170	16
BM	190	26
BM1700	180	26.9
BM1900	180	8.7
WM	190	30.5
WM1700	190	17.8
WM1900	170	8.1

The slight variation in LCTR values observed when additional heat treatments were imposed upon the starting microstructure (BM group) may be attributed to the fact that only minor change to the microstructural homogeneity was attained. Since the material had experienced numerous conventional heat treatments throughout its service history, precipitation of secondary phases had reached a point of near-saturation, minimizing any additional precipitation upon the subsequent heat treatment cycle performed in this study at the same solution temperature. Elevation of the solution temperature above that utilized in this study has demonstrated grain growth, which would tend to negate the beneficial effects of elemental homogenization due to decreased grain boundary surface area and increased liquid film thickness. [10,11]

In the case of weld metal microstructures, the susceptibility to weld metal liquation cracking was reduced only in the samples subjected to a high-temperature (1038 °C) PWHT. This solution temperature was effective in dissolving much of the δ-phase and Laves (in the case of WM1900 samples) and reducing the potentially damaging effects of Nb segregation to grain boundaries. Since the high-temperature PWHT yielded lower LCTR values in both microstructural forms, further tailoring of high-temperature "rejuvenation" heat treatments may present an avenue for improved weldability characteristics of service-exposed material. A more definitive model for δ-phase dissolution and its effect on grain boundary liquation is required before such treatments can be successfully applied.

Conclusions

1. Significant levels of δ-phase were observed in wrought Alloy 718 base and weld metal from actual hardware subjected to multiple repair/PWHT cycles.
2. Little difference in hot ductility behavior was observed between weld metal and wrought base metal microstructures exposed to multiple repair/PWHT cycles.
3. No difference in hot ductility behavior was observed when service-exposed wrought base metal and weld metal was subjected to a single additional PWHT with a 927 °C (1700 °F) solution temperature. Measurable improvement occurred when the solution temperature was raised to 1038 °C (1900 °F).
4. The 1038 °C treatment was successful in dissolving much of the δ-phase and Laves phase constituents in the wrought base metal and weld metal microstructures.

References

1. Sims, C.T., Stoloff, N.S., and Hagel W.C., Superalloys II, John Wiley and Sons, New York, 1987, pp. 27-188, 495-515.

2. Brooks, J.W., and Bridges, P.J., "Metallurgical Stability of Inconel Alloy 718," Superalloys 1988, ed. Reichman, S., Duhl, D.N., Maurer, G., Antolovich, S., and Lund, C., The Metallurgical Society, 1988, pp. 33-42.

3. Benson, J.M., and Blum, F., "The Effect of Rejuvenation Heat Treatments on the Low Cycle Fatigue Performance of IN-718," Specialty Metals Programme Report, 1993, pp. 1-8.

4. Benson, J.M., and Miglietti, W., "Investigation into the Rejuvenation of IN718 By Heat Treatment," Specialty Metals Programme, 1989, pp. 1-25.

5. Koul, A.K., Au, P., Bellinger, N., Thamburaj, R., Wallace, W., and Immarigeon, J.P., "Development of a Damage Tolerant Microstructure for Inconel 718 Turbine Disc Material,"

Superalloys 1988, ed. Reichman, S., Duhl, D.N., Maurer, G., Antolovich, S., and Lund, C., The Metallurgical Society, 1988, pp. 3-12.
6. Radavich, J.F., and Korth, G.E., "High Temperature Degradation of Alloy 718 After Longtime Exposures," Superalloys 1992, ed. Antolovich, S.D., Stusrud, R.W.,MacKay, R.A., Khan, T., Kissinger, R.D., and Klarstrom, D.L., The Minerals, Metals & Materials Society, 1992, pp. 497- 506.
7. Campo, E., Turco, C., and Catena, V., "The Correlation Between Heat Treatment, Structure and Mechanical Characteristics in Inconel 718," Metallurgical Science and Technology, 3 (1985), pp. 16-21.
8. Lin, W., Lippold, J.C., and Baeslack, W.A. III, "An Evaluation of Heat-Affected Zone Liquation Cracking Susceptibility, Part 1: Development of a Method for Quantification," Welding Journal, 1993, pp. 135s-153s.
9. Burke, M.G., and Miller, M.K., "Precipitation in Alloy 718: A Combined AEM and APFIM Investigation," Superalloys 718, 625, and Various Derivatives, ed. E.A. Loria, The Minerals, Metals & Materials Society, 1991, pp. 337-350.
10. Mills, W.J., "Effect of Heat Treatment on the Tensile and Fracture Toughness Behavior of Alloy 718 Weldments," Welding Journal, 1984, pp. 237s-245s.
11. Mills, W.J., "Fracture Toughness of Thermally Aged Alloy 718 Weld Metal," Welding Journal, 1987, pp. 113s-119s.

Acknowledgments

The authors would like to thank General Electric Aircraft Engines and the Federal Aviation Administration (FAA) Aging Aircraft Program for the financial support of this work. The technical input of Mr. Tom Kelly of GE is appreciated. The authors also appreciate the valuable insight on weldability testing provided by Dr. Wangen Lin, formerly with Edison Welding Institute, and currently with Pratt and Whitney.